M. Endo, H. Sugiyama, and A. Rajendran

DOI: 10.1002/anie.201102113

Single-Molecule Analysis

Single-Molecule Analysis Using DNA Origami

Arivazhagan Rajendran, Masayuki Endo, and Hiroshi Sugiyama**

Keywords:
atomic force microscopy · DNA origami · nanodevices · nanotechnology · single-molecule studies

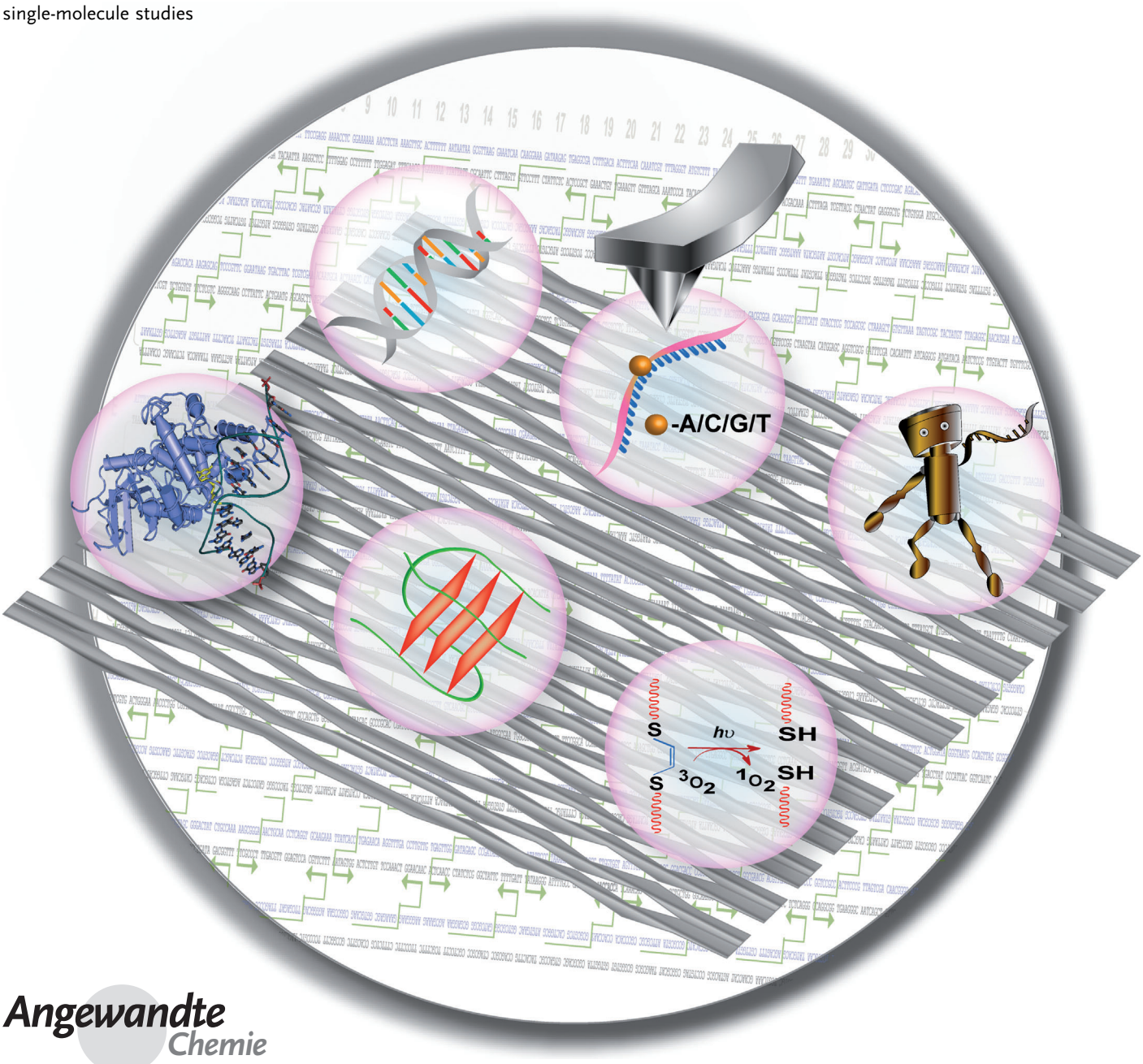

Angewandte International Edition Chemie

During the last two decades, scientists have developed various methods that allow the detection and manipulation of single molecules, which have also been called "in singulo" approaches. Fundamental understanding of biochemical reactions, folding of biomolecules, and the screening of drugs were achieved by using these methods. Single-molecule analysis was also performed in the field of DNA nanotechnology, mainly by using atomic force microscopy. However, until recently, the approaches used commonly in nanotechnology adopted structures with a dimension of 10–20 nm, which is not suitable for many applications. The recent development of scaffolded DNA origami by Rothemund made it possible for the construction of larger defined assemblies. One of the most salient features of the origami method is the precise addressability of the structures formed: Each staple can serve as an attachment point for different kinds of nano-objects. Thus, the method is suitable for the precise positioning of various functionalities and for the single-molecule analysis of many chemical and biochemical processes. Here we summarize recent progress in the area of single-molecule analysis using DNA origami and discuss the future directions of this research.

From the Contents

1. Introduction

Many chemical and biological processes are too complex to be fully understood using conventional ensemble techniques, in which many molecules of one or various species are investigated at the same time. In such a bulk approach (recently, Bustamante termed it "in multiplo"),[1] the changes in the properties of each of the molecules that participate in these transformations sum up to yield a measurable signal. Although these methods are commonly used, they have enormous drawbacks, and, in many cases, seriously fail to reproduce the single-molecule (also termed "in singulo") properties of a system. At the molecular level, most of the processes occur in a discrete and random fashion, and the bulk properties may not represent exactly the properties of each molecule. In principle, all biochemical reactions in vivo occur by the action of single enzymes, nucleic acids (either DNA or RNA), and/or proteins. Thus, single-molecule analysis is necessary to comprehend any chemical or biochemical reaction.

The first single-molecule studies were pioneered about two decades ago.[2] Since then, the application of these methods to an increasing variety of problems has experienced an explosive growth. These methods not only avoid the bulk average, but also allow the trajectories of the individual molecules to be followed as they undergo their reactions in real time. These approaches revealed information on kinetic processes[3] and were successful in several applications, such as gene expression profiling,[4] detection of single-nucleotide polymorphisms (SNPs),[5] structural prediction of biomacromolecules,[6] and drug screening.[7] Most of these studies were performed using picomolar to nanomolar concentrations of fluorophores to isolate the individual molecules in solution. However, many enzymes work at much higher ligand concentrations, and their Michaelis constants are often in the micromolar to millimolar range.[8] Later, methods were developed for single-molecule analysis at high fluorophore concentrations and for its application to enzyme studies.[9]

Rapid progress in nanobiotechnology and efforts aimed at building lab-on-a-chip systems for low-cost, high-throughput analytical biochemistry were concurrent with the development of single-molecule analytical techniques. The field of DNA nanotechnology was pioneered by Seeman, who laid a theoretical framework for the use of DNA as a nanoscale building material.[10] Subsequently, DNA was used in the preparation of increasingly complex shapes and lattices. Since its inception, the single-molecular techniques have gained much attention in the field of structural DNA nanotechnology. The DNA motifs constructed using structural DNA nanotechnology were in the size range of 10–20 nm, which is not sufficient for many practical applications,[11] and the strategies used for the construction of larger assemblies with defined size were limited. Moreover, specific enzymatic

[*] Dr. A. Rajendran, Prof. Dr. H. Sugiyama
Department of Chemistry, Graduate School of Science
Kyoto University, Sakyo-ku, Kyoto 606-8502 (Japan)
Fax: (+81) 75-753-3670
E-mail: hs@kuchem.kyoto-u.ac.jp
Homepage: http://kuchem.kyoto-u.ac.jp/chembio
Dr. A. Rajendran, Dr. M. Endo, Prof. Dr. H. Sugiyama
CREST, Japan Science and Technology Corporation (JST)
Sanbancho, Chiyoda-ku, Tokyo 102-0075 (Japan)
Dr. M. Endo, Prof. Dr. H. Sugiyama
Institute for Integrated Cell-Material Sciences (iCeMS)
Kyoto University
Yoshida-ushinomiyacho, Sakyo-ku, Kyoto 606-8501 (Japan)
E-mail: endo@kuchem.kyoto-u.ac.jp

reactions require the fixation of the system within a nanospace of larger dimension, so that the selective reaction can be monitored unimolecularly.[12] For instance, the DNA methylation enzyme *Eco*RI methyltransferase (M.*Eco*RI) bends double-helix DNA by 55–59° during the reaction.[13] Thus, the enzymatic reaction can occur on the DNA strand that can bend easily during the course of the reaction, whereas the strand that cannot undergo any bending may be less influenced (or not at all) by the enzyme. To monitor such a reaction in real time using nanotechnology, the sequence of interest should be fixed within a DNA motif with some relaxation (so that the strand can bend during the reaction), and a control strand with a nearly identical sequence should be fixed with some tension (no bending is allowed in this case). Such an assembly can be used for the selective methylation of DNA strands. Likewise, the organization of molecular species scaffolding in larger two-dimensional (2D) space with defined spacing between them (like a molecular breadboard) has been a central component of structural DNA nanotechnology.

In 2006, Rothemund[14] developed a versatile and simple method of self-assembly, termed the "scaffolded DNA origami", for the preparation of defined, larger 2D assemblies of almost any arbitrary shape with a diameter of about 100 nm. In this technique, a single-stranded viral genome (M13mp18), which serves as a scaffold, and hundreds of predesigned short oligomers ("staples") hybridize with the scaffold strand through complementary base pairing to form many branched junctions between adjacent helices (Figure 1). A one-pot nanomolar-scale synthesis yields over 10^{14} origami tiles with a yield of nearly 100%. This method has been successfully used for the preparation of various 2D[15] and 3D assemblies[16] and for the nanopatterning of proteins,[17] nanoparticles,[18] and other functional components[19] into well-defined arrangements. These structures can also act as templates for the growth of nanowires, aid in the determination of protein structure, and provide new platforms for genomics applications.[20] Although the origami method was used in DNA nanotechnology, single-molecule analysis was carried out first for the RNA hybridization assay[21] (if we exclude the nanopatterning of functional molecules[17–19]). After this application, the method was used for various single-molecule analyses, ranging from chemical,[22] photochemical,[23] and biochemical reactions[24] to determination of photophysical properties,[25] recognition of SNPs,[26] and conformational changes in DNA.[27] These types of analysis would not have been feasible using short DNA motifs.

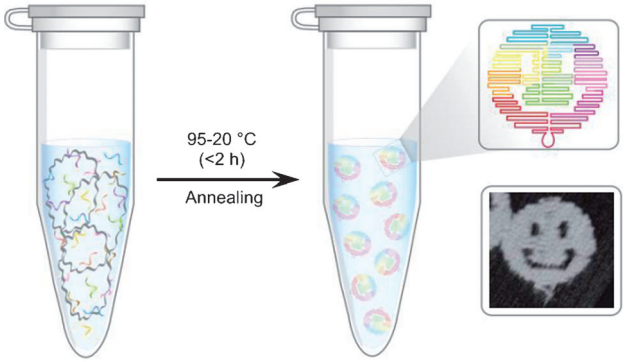

Figure 1. Drawing of the preparation of a smiley-shaped origami structure and its AFM image. Gray and color ribbons in the left-hand tube represent the M13 mp18 and staple strands, respectively.

Single-molecule methods can be broadly classified into two major categories: 1) fluorescence imaging and spectroscopy; and 2) force-based techniques. Among the force-based techniques, atomic force microscopy (AFM) is used mainly for single-molecule analyses in nanotechnology and can even be used for all origami-based studies. Few reports describe the use of the fluorescence-based techniques for this purpose.[28] Herein, we focus on the single-molecule analysis using DNA origami, which is a method used for the isolation of single molecules and for their analysis, in combination with the available unimolecular techniques.

2. Label-Free Single-Molecule Biomolecular Recognition

One of the most important features of DNA origami is that each position on the 2D surface contains different sequence information. Therefore, the sequence carrying functionality can be placed anywhere on the 2D structure in a targeted fashion. For example, a nanoparticle-conjugated sequence can be complementarily hybridized with the M13

Arivazhagan Rajendran received his BSc in Chemistry from the Government Arts College, Krishnagiri (Periyar University, Salem), in 2001 and an MSc from the University of Madras (India) in 2003 specializing in inorganic chemistry. He then began PhD research in Bioanalytical Chemistry working with Norio Teramae at Tohoku University (Japan). After receiving his PhD in 2008, he joined the Frontier Institute for Biomolecular Engineering Research (FIBER) at Konan University as a postdoctoral researcher. He recently moved to the Institute for Integrated Cell-Material Sciences (iCeMS) at Kyoto University.

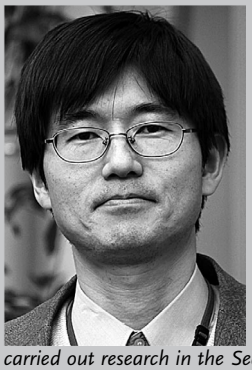

Masayuki Endo graduated from Kyoto University (I. Saito) and received his PhD at the University of Tokyo (M. Komiyama) in 1997. He moved to Tokyo Medical and Dental University (under the direction of H. Sugiyama) as a JSPS postdoctoral fellow. He continued research in the Verdine group at Harvard University as a postdoctoral fellow (1998–2000). After working in the Yokoyama group at RIKEN, he joined the Institute of Scientific and Industrial Research, Osaka University, as an Assistant Professor (2001–2008). During this time, he carried out research in the Seeman group (New York University, 2005) as a visiting scholar. Since 2008, he has been in the Sugiyama group at iCeMS, Kyoto University, as an Associate Professor.

scaffold, which can position the particle on the surface of the origami. Furthermore, the single-stranded protrusion of the DNA of a specific sequence can be placed on the origami, which can be used as a receptor for its complementary DNA or RNA sequence. In principle, any functionality that can be conjugated with DNA can be placed on the surface of the origami and serve as a probe for molecular recognition. This is how the origami method isolates single molecules that can be investigated using a suitable single-molecule technique. To keep them perpendicular to the 2D plane, probes should be placed at a position eight base pairs away from the crossover, which defines a spatial resolution of about 6 nm between any two probes. This renders any system with two or more components that can be isolated and placed with a defined space between the components, suitable for the analysis of any distance-dependent property. Moreover, one hundred trillion probe tiles are fabricated in a single step and within one hour, which renders the method suitable for practical applications.

2.1. RNA Hybridization Assays

The study by Ke et al. in 2008[21] can be considered the first single-molecule analysis of biomolecules, although single molecules or particles had been placed on a DNA origami nanostructure and characterized using the AFM technique before. The authors developed an assay for label-free RNA hybridization on the DNA origami, which is a molecular analogue of macroscopic DNA chips. Single-stranded DNA segments with a length of 20 nucleotides, complementary to the RNA target and acting as probes, were placed on the origami (Figure 2A). The recognition/hybridization process was carried out unimolecularly and imaged using AFM. After hybridization of the target to a pair of half probes, the DNA–RNA hybrid formed a V-shaped structure (Figure 2B) that can be easily visualized as a bright spot on the AFM image.

Therefore, the method does not require labeling of the target and/or probe sequences, and recognition at the single-molecule level can be readily visualized. The assay was extended to the simultaneous recognition of multiple RNAs corresponding to a region of three genes, *Rag-1*, *c-myc*, and *β-actin*, that are expressed in the murine progenitor B cell line

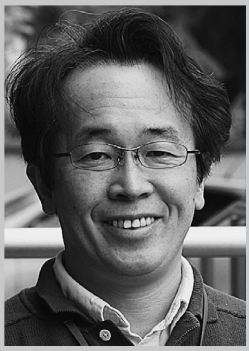

Hiroshi Sugiyama received his PhD in 1984 with T. Matuura at Kyoto University. After postdoctoral studies at the University of Virginia with S. M. Hecht, he returned to Kyoto University in 1986 as an Assistant Professor and became an Associate Professor in 1993. In 1996, he joined the Institute of Biomaterials and Bioengineering at Tokyo Medical and Dental University. He has been a Professor of Chemical Biology at Kyoto University since 2003. Among the honors he has received are the Nippon IBM Award and the Chemical Society of Japan Award for Creative Work.

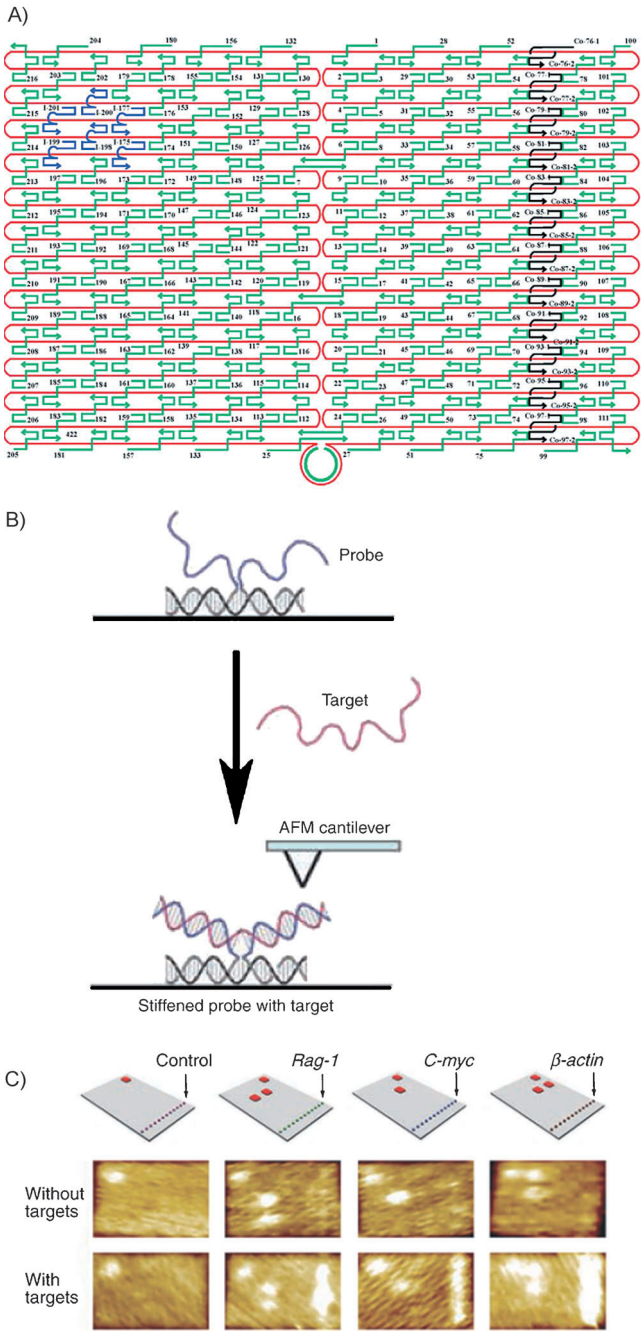

Figure 2. Recognition of target RNA by hybridization with probe DNA strands introduced on a DNA origami structure. A) Representation of the origami with probe strands on the right (black) and index hairpins at the top left corner (blue). Red and green lines indicate the M13mp18 scaffold and staple strands, respectively. B) A pair of neighboring helper strands protrude out of the origami surface, with each 20 nucleotide long extension bearing half of the target RNA sequence. These protrusions do not produce a visible feature in the AFM image. However, upon hybridization with the target, it produces a V-shaped junction that is readily visible as a bright spot in the AFM image. C) Topographic illustration of the bar-coded tiles and the corresponding AFM images in the absence and presence of targets. Specific target recognition can be identified by the corresponding index.

(Figure 2C). The origami tiles carrying DNA sequences that were complementary to the above-mentioned RNA sequences, which were indexed with barcode hairpin markers, were mixed, and binding to the target was carried out. Even though the different probe tiles were mixed together, specific binding of the target was achieved, as characterized using the barcode markers. Furthermore, the effectiveness of the method in recognizing the target was confirmed in the presence of a large amount of cell-derived RNA, in which no nonspecific recognition was identified. Although this approach cannot compete with existing technologies, such as microarrays[29] and the reverse-transcription polymerase chain reaction,[30] which analyze thousands of targets simultaneously, the present method may ultimately permit the detection of low levels of gene expression, possibly down to the single-cell level. In support to this, it has been demonstrated that the DNA origami structures retain their structure and remain folded against nuclease digestion[31] and in cell lysate.[32] Thus, it is possible to use these structures in cell level, if single cell gene expression detection and proteomics are to be realized. Arguably, further developments are necessary to achieve this goal.

2.2. Distance-Dependent Aptamer–Protein Binding

The advantage of structural nanotechnology is the assembly of multiple molecules while controlling the spacing between them, which renders the method suitable for distance-dependent single-molecule analyses, such as molecular recognition. The importance of the origami method for single-molecule analysis was best illustrated in the label-free investigation of distance-dependent aptamer–protein binding.[33] As shown in Figure 3A, a DNA origami tile was designed to display two different protein-binding aptamers (short oligonucleotide sequences), with precise control over the distance between them. These aptamers bind to sites on almost opposite sides of a coagulation protein, thrombin, which is a key promoter of blood clotting. The size of the protein is about 4 nm and a gel-mobility shift assay revealed that it can bind to aptamers placed 5.3 nm apart from each other. At larger or smaller distances, either no or low binding was observed. Protein recognition on the origami surface was characterized using AFM. As designed, the protein bound to heteroaptamers that were kept at a distance of 5.8 nm from each other, whereas no recognition was observed when this distance was 20.7 nm (Figure 3C). The possibility of positional effects caused by electrostatic repulsion between the protein and the DNA scaffold was ruled out, as shown in Figure 3B,D. The DNA origami method presents an advantage over the bulk approaches because in the latter, the aptamers cannot be fixed at an optimal distance. The method can also be extended to a variety of multicomponent bimolecular interactions, which can be visualized at a single-molecule level.

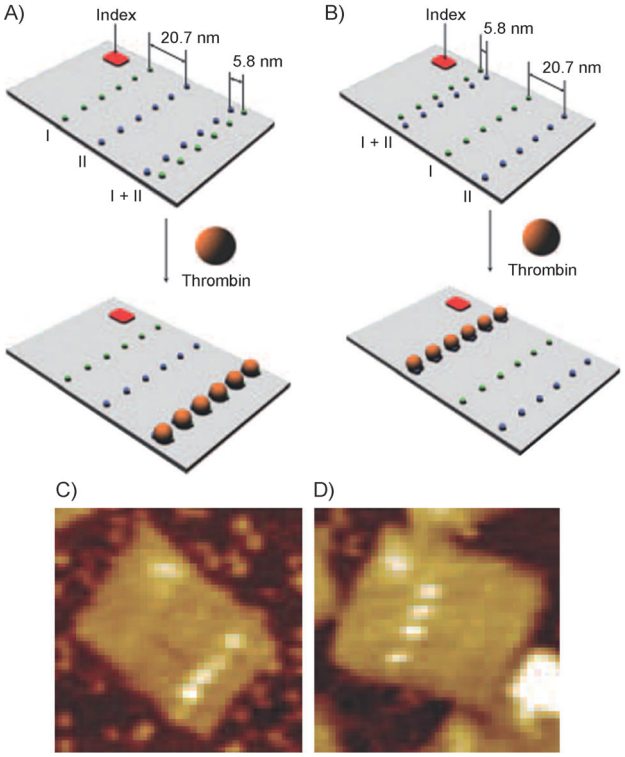

Figure 3. Drawing of the DNA origami tile with a hairpin index marker at the top left corner, and two lines of aptamer apt-I (green dots) and two lines of apt-II (blue dots). The positional effect was studied in two different ways, (A) and (B), by changing the distance of the neighboring lines of apt-I and apt-II. The protein recognition in each case is also shown. AFM images of the protein binding corresponding to the schemes (A) and (B) are given in (C) and (D), respectively. Each image corresponds to a size of $150 \times 150\ nm^2$.

2.3. Single-Nucleotide Polymorphism Detection

One of the first goals of the extraction of medical and biological information from the human genome was the study and exploitation of the single-letter changes in the DNA code.[34] These variations are the major basis of phenotypic individuality and genetic variation, and might signal vulnerability to, or protection from, ailments such as cancer, heart disease, and diabetes. Although many methods of SNP detection exist,[35] there is no one accepted technology of choice.

Subramanian et al.[26] attempted to show the ability of DNA nanotechnology to detect SNPs unimolecularly. The method combined the AFM technique with DNA origami patterns to produce a direct visual readout of the target nucleotide present in the probe sequence. The origami was designed to contain the graphical representations of all four nucleotide alphabetic characters (Figure 4A); furthermore, the symbol containing the test nucleotide identity vanishes after the addition of the probe sequence. In this approach, the working principle of SNP detection incorporates the kinetic method based on branch migration, which was used successfully in solution-state in multiplo SNP analysis.[36] The interesting feature of this system is that it works isothermally, so that the progression of branch migration is ultimately

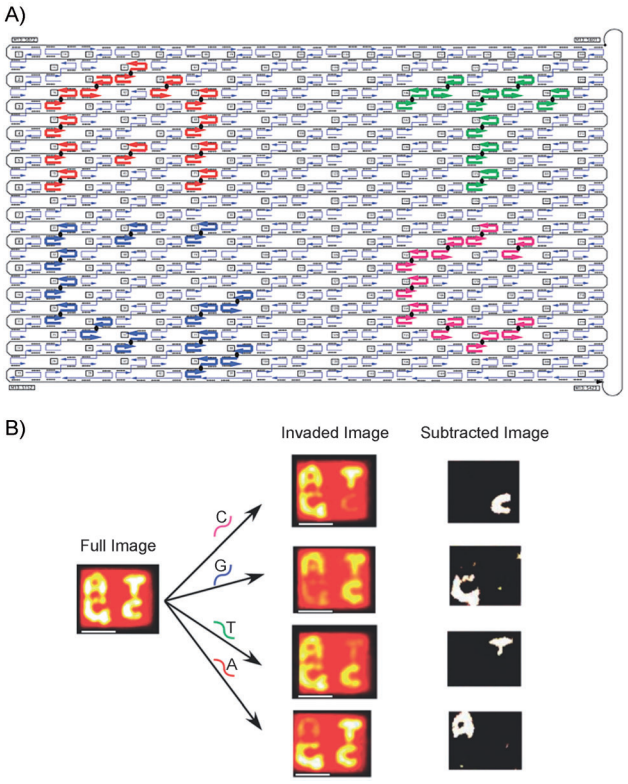

Figure 4. A) The DNA origami tile used for SNP detection. Black, thin blue, and thicker lines represent the M13 scaffold, staple strands, and strands involved in producing the letters, respectively. B) Operation of the SNP detection system. The full image shows an AFM image of the origami tile before invasion. The four invaded images correspond to the averaging of 25 separate AFM images, and the identity of the key nucleotide in the invasive strand is indicated over the arrow. The scale bars represent a distance of 50 nm. The subtracted image reveals the identity of the nucleotide.

unidirectional, from the toehold region to the opposite end. In addition, a photocleavable linker that breaks upon irradiation is incorporated into the system. Thus, the signal-producing component is readily bound to the origami after the initial assembly, but may then be freed, so as to be released by the probe strand. A computer analysis of a set of AFM images produced a direct readout of the nucleotide present in the probe (Figure 4B). The system also works with pairs of probes, corresponding to the heterozygous diploid genomes. Interestingly, the kinetic process of the strand exchange is not inhibited because of the immobilization of the system on the origami scaffold.

The whole sequence of a synthetic oligomer, and not only single nucleotides, can be recognized using the origami method.[37] The recognition of a single DNA sequence was demonstrated with AFM using the biotin–streptavidin complex as a pixel-contrast-enhancing marker. In this case, a linear probe was employed rather than a V-shaped probe, which led to a much smaller positional effect. Although a set of probe sequences was used in all the cases mentioned above, in principle, single-probe sequences are sufficient for unimolecular recognition.

3. Conformational Analysis

The method can also be extended to the conformational analysis of biomolecules. Conformational changes in the DNA of living systems are closely associated to the regulation of their biological functions, such as gene expression. Many human sequences have the potential to adopt non-B conformations. Genes harboring the non-B DNA structure-forming sequences are associated with an increased risk of genetic instability, and are thus associated with human diseases.[38]

3.1. Human Telomeric G-Quadruplexes

Among the conformations of DNA, the G-quadruplex structure is of great interest because of the large abundance of G-rich repeated sequences at the telomeric region of the human genome.[39] The G-quadruplexes formed by the G-rich strands are promising anticancer targets, as formation of such structures inhibits the activity of telomerase.[40] The structure of human telomeric G-quadruplexes is the subject of intense research,[41] but still remains puzzling.

We developed a novel method using an origami nanoscaffold for the label-free direct observation of the formation of single G-quadruplex structures under conditions that favor the folding of a four-stranded structure, and of its disruption under unfavorable conditions.[27] As shown in Figure 5A, a DNA origami frame structure with an inner vacant rectangular area was constructed in which two sets of connection sites were introduced for the hybridization of duplex DNAs of interest. Each duplex DNA contained a single-strand G-rich protrusion, with three G-tracts in the upper and one G-tract in the lower strand. In the absence of K^+, the G-tracts do not form a quadruplex structure and the duplex strands adopt a parallel conformation. In contrast, addition of K^+ forces the protrusions to form the $(3+1)$ G-quadruplex, which can be monitored by visualization of the X shape of the introduced strands. As expected, we were able to monitor the conformational change of the G-tracts from the single-strand to the G-quadruplex form and vice versa at the single-molecule level (Figure 5B,C). The success of our method lies not only on the static observation of the changes, but also on the possibility of following the trajectories of the formation or disruption of a single G-quadruplex structure as it undergoes conformational change in real time. This type of real-time analysis of the formation of a $(3+1)$ G-quadruplex in the presence of K^+ is illustrated in Figure 5D. The strands initially form the parallel state, and, after a certain time, convert into an X shape, which is clear evidence of the formation of a four-strand structure. The sequence dependence of the formation of the X shape was also investigated using a variety of sequences. The method can be extended to the various conformational changes of nucleic acids.

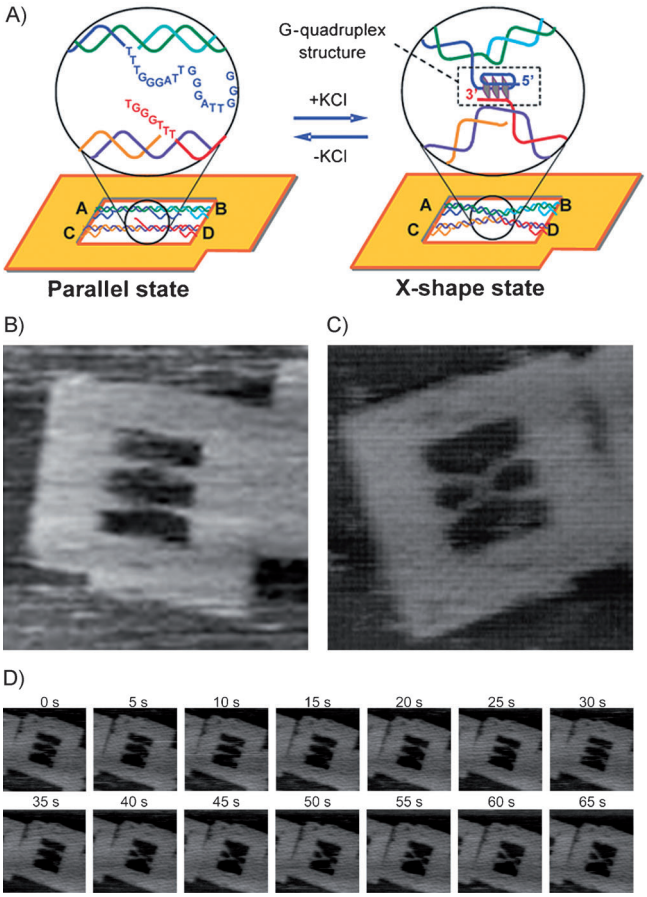

Figure 5. A) Representation of a DNA frame with G strands forming a parallel shape and an X shape in the absence and presence of K^+, respectively. AFM images of the corresponding shapes are given in (B) and (C). D) A snapshot of the fast-scanning AFM images of the G-quadruplex formation event. The image sizes are 170×170 nm^2 for (B) and (C) and 160×160 nm^2 for (D).

3.2. The Secondary DNA Binding Site in Human Topoisomerase I

Human topoisomerase I (hTopoIB) is a typical representative of the nuclear forms of the eukaryotic type IB topoisomerases. It is a 91 kDa monomeric enzyme that controls and alters the topological states of DNA during transcription. This enzyme catalyzes the transient breaking and rejoining of single-stranded DNA, which allows the strands to pass through one another, thus altering the topology of DNA. It is believed that hTopoIB binds only one site on the DNA helix at a time. However, it was recently suggested that the existence of a secondary DNA-binding domain in the enzyme allows the simultaneous interaction with two DNA sites.[42] There may be two types of secondary interactions between hTopoIB and DNA: 1) simultaneous interaction of one TopoIB with two DNA helices (interaction mode T_1); and 2) interaction between two cleavage complexes of TopoIB-DNA (interaction mode T_2). However, the existence of a secondary binding site in nuclear type IB topoisomerases has never been addressed directly.

Subramani et al.[43] attempted to unravel the secondary DNA binding sites in topoisomerase I using the DNA origami method. The strategy is outlined in Figure 6A. A rectangular DNA origami with a bait DNA protrusion at a selected position was prepared by extending one of the short single-strand DNA (staple strands) with a stretch of 21 nucleotides, which was then hybridized with a complementary sequence. The secondary interactions described above were studied by adding either the TopoIB-DNA complex (T_1 mode) or by stepwise addition of the TopoIB and cleavage complex (T_2 mode) to the origami with bait DNA, which was immobilized on a mica surface. The binding process was monitored using AFM.

As shown in Figure 6B, the protruding bait DNA was not visible in the AFM image because of the flexibility of double-stranded DNA. In contrast, the addition of the purified cleavage complex resulted in a bright spot on the DNA

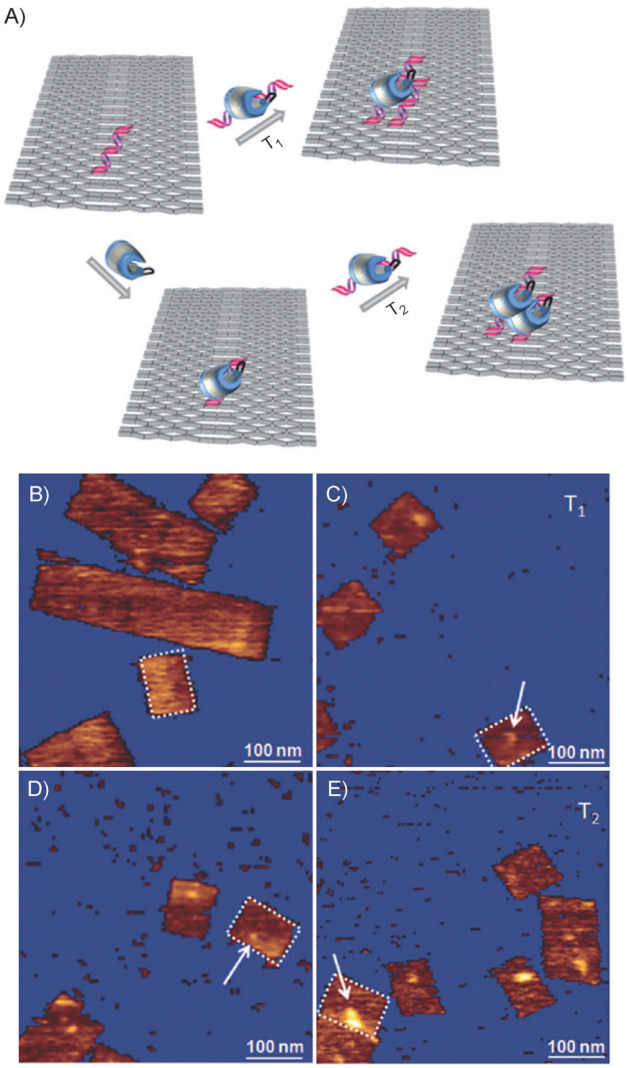

Figure 6. A) Experimental setup for investigating the interactions of bait DNA on origami with an hTopoIB–DNA cleavage complex (T_1 interaction mode, top) and stepwise interaction between two cleavage complexes (T_2 interaction mode, bottom). B)–E) AFM images of the DNA origami with bait DNA (B), after incubation with the cleavage complex (C), incubated with hTopoIB (first step of T_2 mode (D), and subsequent addition of the cleavage complex (second step of T_2 mode; (E)).

origami where the bait DNA was located (arrow in Figure 6C). This spot was identified as representing the interaction between the bait DNA and the cleavage complex, suggesting the presence of a T_1 secondary interaction mode. Similarly, the treatment of the origami with TopoIB resulted in a bright spot (arrow in Figure 6D), indicating the presence of a bait DNA–TopoIB interaction. The spot became much brighter after the subsequent addition of the cleavage complex (arrow in Figure 6E). This is clear evidence of a T_2 interaction mode. The results presented strongly support the existence of a secondary DNA binding site in this enzyme. Such a site may provide DNA crossover recognition potential to the enzyme, which in turn may function as a topological sensor, directing hTopoIB action to plectonemic supercoiled DNA.

4. Chemical Reactions

Biomolecules, such as nucleic acids and proteins, are relatively large; therefore, they can be readily visualized using AFM, whereas components that are involved in a chemical reaction are too small for detection. Nevertheless, a stunning demonstration of the advantages of the use of DNA origami for single-molecule analysis of chemical reactions was recently reported by Voigt et al.[22] The authors used origami structures as an addressable support to achieve and visualize the cleavage and formation of individual chemical bonds.

4.1. Bond-Cleavage Reactions

Rectangular DNA origami was prepared using biotinylated staple strands at 12 different positions to demonstrate bond-cleavage reactions. The addition of streptavidin leads to the formation of a strong complex with biotin, which was used as a readout of the chemical reaction. Three different types of linkers were incorporated into these biotin-conjugated staple strands: noncleavable linkers (type A, which work as a reference), linkers containing a disulfide moiety (type B, which can be cleaved by a reduction reaction), and linkers containing an electron-rich 1,2-bis(alkylthio)ethene moiety (type C, which can be cleaved by singlet oxygen). Efficient cleavage of linkers B and C was performed using 1,4-dithiothreitol, and singlet oxygen photosensitized by eosin, respectively (Figure 7A). These reactions were monitored at the single-molecule level using AFM to study the selective disappearance of streptavidin from the surface of the DNA origami.

4.2. Bond-Formation Reactions

Single-molecule recognition of the formation of a chemical bond is an even more difficult task, as the location of the attachment point often remains unknown until the reaction occurs. However, the DNA origami method offers a suitable platform to address this issue, as the exact position of the reacting functional group can be predetermined on the origami template. One of the reacting groups can be placed on the surface of the origami and the incoming group can be linked to biotin. Incorporation of the functional group or formation of the chemical bond can be visualized by the addition of streptavidin. The reactions of three functional groups (alkyne, amine, and azide) were studied. These groups are commonly used in bioconjugation reactions. An alkyne can react with an azide and vice versa in a Huisgen–Meldal–Sharpless azide–alkyne click reaction[44,45] to form a triazole, and an amine can react with an *N*-hydroxysuccinimide-activated ester to form an amide moiety. These reactions proceed successively on the immobilized origami platform with a high degree of chemoselectivity (Figure 7B). This would represent the emergence of a new type of "single-molecule chemical synthesis" that can be highly selective. Furthermore, it would be possible to use this method to study a variety of chemical reactions and processes.

4.3. Photochemical Reactions

The photochemical reaction, namely bond cleavage by singlet oxygen formed by photosensitization, was described in the previous section. In that case, the singlet oxygen was produced in the bulk solution and was used for bond cleavage on the surface of the DNA origami. The production of singlet oxygen at the single-molecule level and its behavior on the origami template is very attractive. This type of investigation was reported recently.[23] A single indium pyropheophorbide singlet-oxygen photosensitizer (IPS) was conjugated to a staple strand located in the middle of the origami tile. To monitor the behavior of singlet oxygen, biotinylated oligonucleotides containing a singlet-oxygen-cleavable linker were placed at both sides of the photosensitizer-conjugated strand (Figure 8A). Furthermore, a biotinylated reference strand was placed in a corner. Similar to the previous case, the biotin–streptavidin complex was used as readout of the reaction. The production of singlet oxygen by a single photosensitizer and its diffusion within the surface of the origami was successfully characterized using AFM (Figure 8B).

4.4. Azide–Alkyne Click Reactions of Modified Dendrimers

Further to the above-mentioned reactions, DNA-templated covalent coupling of the alkyne- and azide-modified dendrimers was demonstrated on DNA origami.[46] Fourth-generation polyamidoamine–succinamic acid dendrimers (G4-COOH) that were surface functionalized with azides or alkynes and conjugated to a specific DNA strand were used in an azide–alkyne click reaction. This dendrimer had 64 carboxylic acid surface groups and a diameter of about 5 nm. The dendrimer was first modified at the 64 carboxylic acid groups to generate all-azide (G4-azide) or all-alkyne (G4-alkyne) dendrimers. The 1:1 DNA–dendrimer conjugates were prepared using two different 20-nucleotide single-stranded DNAs by a click reaction with one of the 64 surface groups. The remaining 63 surface groups on these conjugates

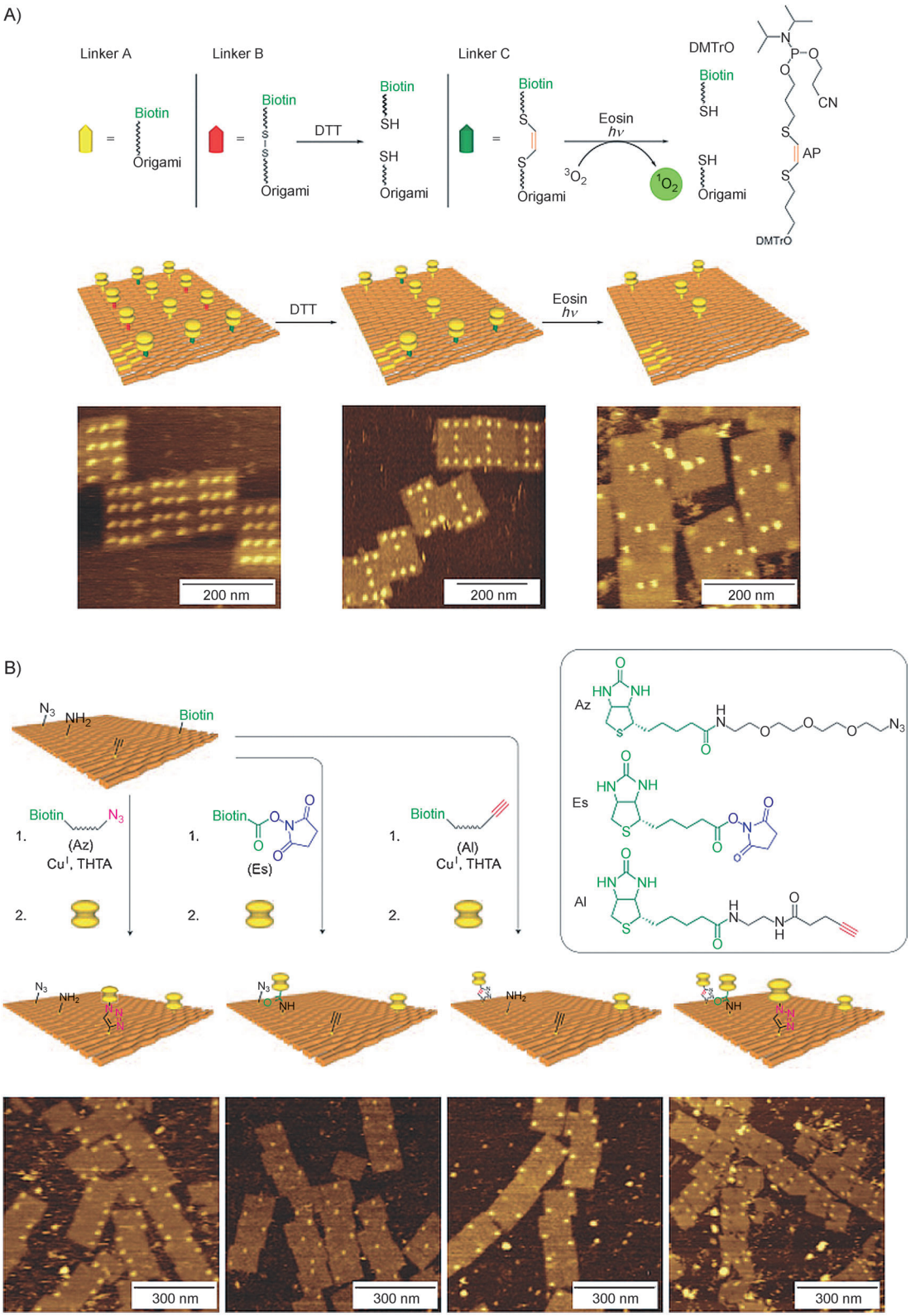

Figure 7. Single-molecule chemical reactions on an origami surface. A) Demonstration of single-molecule analysis of chemical bond cleavage reactions. The selective bond cleavage was detected with AFM after the selective disappearance of bright spots caused by the streptavidin–biotin complex. AP = alkene phosphoramidite, DMTr = 4,4-dimethoxytrityl, DTT = 1,4-dithiothreitol. B) Single-molecule analysis of chemical bond formation. Incoming groups were linked to biotin and the bond formation was monitored using AFM imaging after the addition of streptavidin. Al = alkyne, Az = azide, Es = *N*-hydroxysuccinimide activated ester, THTA = tris[1-(3-hydroxypropyl)triazolyl-4-methyl]amine.

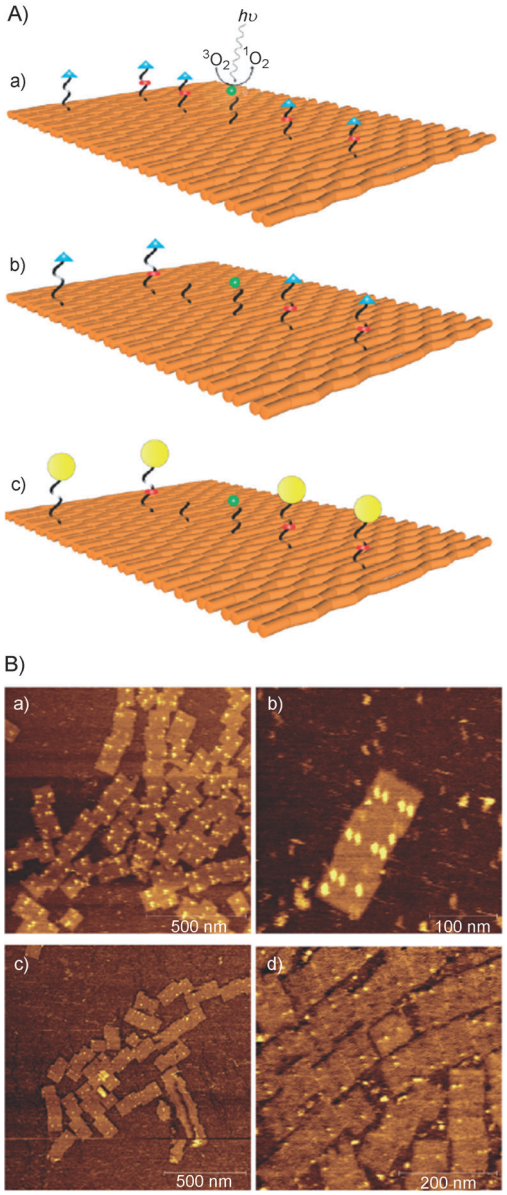

Figure 8. A) Representation of a molecular system: a) Origami during irradiation, b) singlet oxygen reaction at the neighboring strand, and c) origami after irradiation and the addition of streptavidin. B) AFM images of the system: a) Origami structures before irradiation, b) enlarged image without irradiation, c) after irradiation, and d) after irradiation with external IPS.

remained as azide or alkyne groups and were suitable for further coupling reactions on DNA origami. DNA–G4 conjugates containing biotin groups on the G4 surface were synthesized for AFM measurement. A rectangular origami was prepared that consisted of 10 staple strands with two different 20-nucleotide single-strand DNA overhangs around the center of the origami, forming a ring pattern. These overhangs hybridized with the two kinds of DNA-G4 conjugates alternatively (Figure 9A). An AFM image of this origami structure clearly showed the presence of a ring at its middle (Figure 9B, left). The subsequent binding of streptavidin to the dendrimer ring on the immobilized

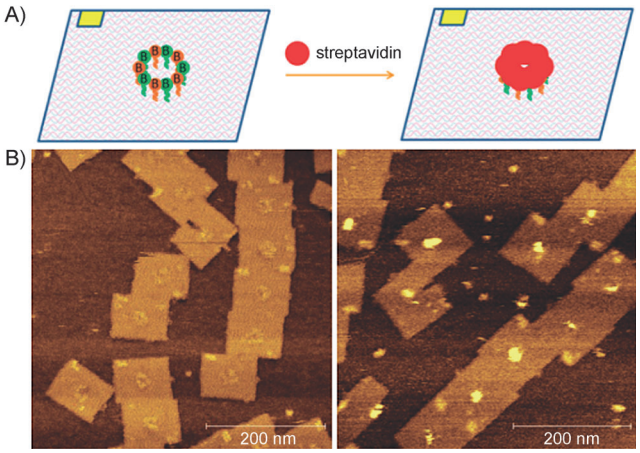

Figure 9. Hybridization of biotin-labeled DNA-G4 conjugates on a DNA origami template and binding of streptavidin. A) The design strategy. B) AFM image of the origami with biotin-modified dendrimers before (left) and after (right) streptavidin binding.

origami was imaged by AFM (Figure 9B, right), and a large height increase (ca. 4 nm) was observed, providing strong support for the presence of dendrimers on the surface of the origami. The covalent coupling of alternating azide and alkyne G4 dendrimers on the surface of the origami using the click reaction was also attempted, and a rough indication of coupling was obtained by gel electrophoresis.

5. Enzymatic Reactions

Enzymes first bind to a nonspecific site, diffuse along the DNA to search for specific sequences, and then react or modify the corresponding sites.[47] Direct observation of these dynamic instances of the interaction of enzymes with DNA may be one of the ultimate goals of the investigation of the mechanical behavior of enzymes during reactions. Structural changes, such as bending of the double-stranded DNA, are often required for the enzymatic reaction to proceed. To perform a selective enzymatic reaction on a particular sequence, it becomes necessary to control the bending of the DNA strand artificially. Using the DNA origami method, we prepared a versatile scaffold that can structurally control the double-stranded DNAs, such as shown in Figure 10A.[12] A structurally tensed 64-mer strand and a relaxed 74-mer strand were incorporated directly to the seam of the M13 scaffold at the positions marked as I/II and III/IV, respectively. The activity of the M.*Eco*RI modifying enzyme was studied. In the presence of *S*-adenosyl-L-methionine (SAM), this enzyme introduces a methyl group at the N6 position of the second adenine of the GGAATC sequence. As DNA methylation proceeds, M.*Eco*RI bends the double helix by 55–59°, flipping out the second adenine.[13] The relaxed strand undergoes bending during the binding of the enzyme and represents a better substrate for the enzymatic reaction. In contrast, the tensed strand is less affected by the enzyme, as it does not bend easily during the enzymatic interaction. Furthermore, after the methylation step, the relaxed strand

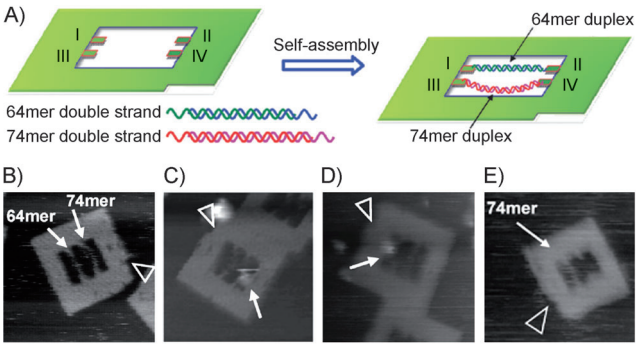

Figure 10. A) Representation of an origami frame and the incorporation of two different structurally controlled DNA strands. B) AFM images of the origami frame with two duplexes, C,D) single M.*Eco*RI binding to the 64-mer (C) and 74-mer (D) strands, and E) the reaction product of successive enzymatic treatment. Restriction enzyme selectively cleaves the 64-mer strand. Image sizes are 225×225 nm^2 (B–D) and 250×250 nm^2 (E).

may not be cleaved by the restriction enzyme (R.*Eco*RI), whereas the nonmethylated tensed strand can be digested. Our fast-scanning AFM analysis performed after successive enzymatic treatments revealed that the 74-mer strand was not effectively cleaved compared with the 64-mer DNA strand, indicating that structural control defines the substrate used for methylation (Figure 10 B–E). Real-time observation of the enzyme binding on the incorporated DNA strands was also demonstrated.

Furthermore, the reactivity of the base-excision repair enzymes 8-oxoguanine glycosylase (hOGG1) and T4 pyrimidine dimer glycosylase (PDG) was studied using a similar strategy of structural control.[24] We also investigated the reaction intermediates of both reactions, which form a covalent bond with the enzyme by reduction with $NaBH_4$. This label-free single-molecule analysis of the enzymatic reactions and reaction intermediates may provide insight into the biological reactions that occur at the single-molecule level inside the cell.

6. Single-Molecule Fluorescence Studies

The ability to study events at the single-molecule level using DNA origami extends beyond chemical and biochemical reactions. In all of the cases discussed above, the moment of a matter (molecule) was monitored at the single-molecule level by using imaging techniques. For instance, in the case of chemical bond formation and dissociation, attachment or detachment involves the displacement of the streptavidin–biotin complex. This is the case even for molecular recognition, which included the monitoring of the movement and attachment of a nucleic acid strand or of a protein. However, physical or photophysical phenomena do not involve such a moment of a matter or a molecule. For example, the energy-transfer process leads to a transfer of energy from the donor to the acceptor, and not the molecule. Monitoring such a physical process on single molecules is a very difficult but most interesting part of DNA origami research.

6.1. Controlled Energy-Transfer Pathways

In a recent study, Stein et al.[25] achieved a combination of multistep energy transfer in a photonic wire-like structure using an energy-transfer cascade. Fluorophores that allow alternative energy-transfer pathways to proceed, depending on the incorporation of jumper dye, were arranged on an origami surface, as shown in Figure 11 A. An input dye (ATTO488), two output dyes (red fluorophore ATTO647N and IR fluorophore Alexa 750), and two jumper dyes (ATTO565) were spread over three helices to minimize fluorophore interactions throughout the DNA molecule. The

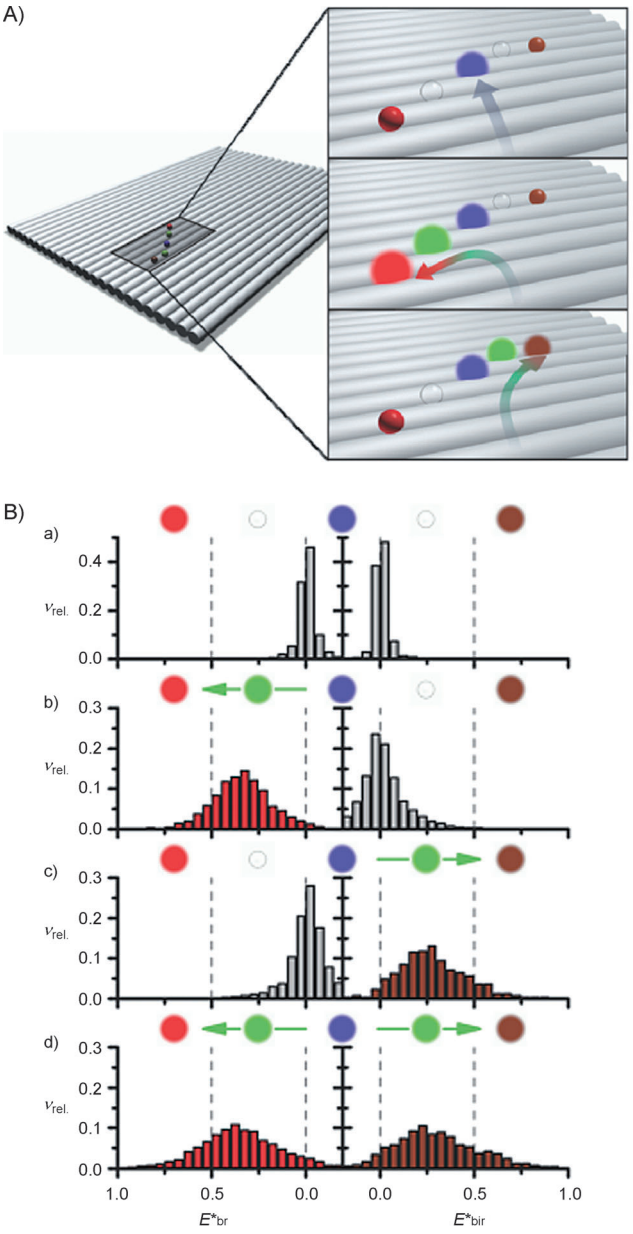

Figure 11. A) Arrangement of fluorophores on DNA origami. B) FRET-related ratios from blue to red, E^*_{br}, and from blue to IR, E^*_{bir}, for the four different origami samples. Blue, green, and red spheres represent the input, jumper, and output dyes, respectively. Colorless spheres indicate the absence of jumper dye.

jumper dyes were placed between the input and output dyes. The single-molecule four-color fluorescence resonance energy transfer (FRET) approach with alternating laser excitation was used in this study, as it seems a better method compared with the force-based techniques. As designed, the energy-transfer pathways from blue to red or blue to IR dyes were successfully controlled at the single-molecule level by the presence of the jumper dyes, which directed the excited-state energy from the input dye to either of the output dyes (Figure 11 B). These results indicate that the DNA origami might serve as a circuit board for photonic devices beyond the diffraction limit and down to the molecular scale.

6.2. A Nanoscopic Ruler for Single-Molecule Imaging

Recent developments in far-field fluorescence microscopy below the diffraction limit have resulted in the production of structures in the sub-200 nm scale, thus making them suitable for optical analysis.[48] To measure the distance between the fluorescent dyes precisely, the optical resolution of these superresolution microscopic techniques needs to be calibrated. Inhomogeneous filamentous structures, such as actin filaments or microtubules and short duplex DNA molecules, are commonly used to demonstrate optical resolution, but are disadvantageous because of their nonnegligible flexibility.[49] Therefore, a defined standard is required, and it should be easily immobilized on the surface in a fixed orientation. DNA origami offers a novel nanostructure with features of precise addressability, defined size, and easy immobilization, and which can be used in single-molecule analyses. These features turn origami structures into a nanoscopic ruler for the calibration of superresolution techniques, as demonstrated recently.[28a] Different superresolution methods, such as single-molecule high-resolution imaging with photobleaching (SHRImP), direct stochastic optical reconstruction microscopy (dSTORM), and blink microscopy, have been used to demonstrate that fluorescently labeled staple strands bound at specific positions of a rectangular origami exhibit a defined separation. Cy5 or ATTO655 were used as fluorophores in the dye-modified staple strands at their 5' end. As shown in Figure 12 A, these dye-modified strands were placed in the lower-left and upper right corners of the origami structure, with a space of 89.5 nm between them. The immobilized samples were imaged using total internal reflection fluorescence (TIRF) microscopy. The emission patterns of the two fluorophores overlapped in the diffraction-limited image, as assessed by TIRF (Figure 12 B). However, superresolution imaging using blink microscopy allowed the identification of the positions of individual fluorophores (Figure 12 C), and the measured distance between the dyes was in good agreement with the original positioning on the DNA origami (Figure 12 D). This origami nanoscopic ruler was also used for the single-molecule imaging and calibration of other superresolution imaging techniques, such as SHRImP and dSTORM.

Along with the 2D origami ruler, a rigid 3D DNA origami ruler was also used in single-molecule FRET spectroscopic analysis.[50]

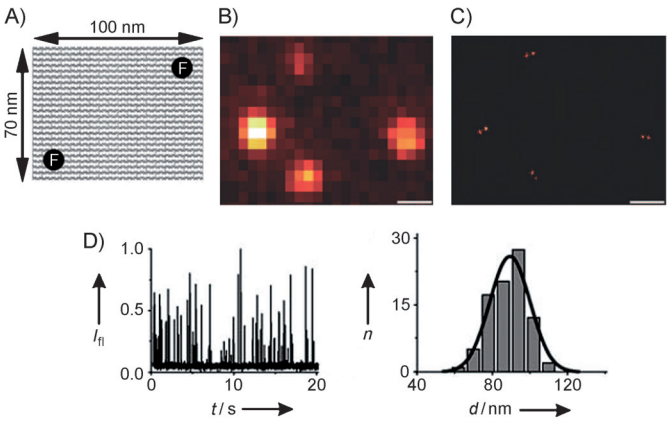

Figure 12. A) Origami tile with two fluorescently labeled staple strands (F in black circle). B) TIRF image of origami tiles each containing two ATTO655-labeled staple strands. C) Super-resolution image of the same region using blink microscopy. D) Intensity versus time profile (left) and the statistical distribution of the measured distance (right). Scale bar: 500 nm.

6.3. Kinetics of Binding and Unbinding Events

High-speed AFM offers a novel imaging method that can record 15 images per second. However, better methods for monitoring the dynamic processes and determining the kinetics in the subsecond range are required. To this end, fluorescence microscopy was successfully applied to the study of the dynamic process of DNA binding and dissociation and to the study of its kinetics in single molecules.[28b] A simple design was used for kinetic analysis that adopted a long rectangular 2D origami structure with a green label dye (ATTO532) incorporated at a corner and a docking strand positioned in the middle (Figure 13 A). The addition of imager strand modified by a red dye (ATTO655) led to the formation of a duplex with the complementary docking strand (Figure 13 B). The formation of the duplex structure was monitored, and the kinetics of the binding and unbinding events were estimated (Figure 13 C). The association rate, which was dependent on the concentration of the imager strand and independent of the duplex length, was determined to be $2.3 \times 10^6\ L\,mol^{-1}\,s^{-1}$ (for 600 mM NaCl), which is comparable with the results of bulk measurements. In contrast, the dissociation rate was independent of the concentration, but strongly dependent on the length of the duplex formed by the imager and docking strands. The dissociation rate was estimated at $1.6\ s^{-1}$ and $0.2\ s^{-1}$ for nine and ten base pairs, respectively. This study explains that, along with the static analysis, the dynamic processes in the subsecond range can be investigated on the DNA origami in real time and are comparable with the results of ensemble measurements.

7. Cargo Transporters and DNA Robots

The function of artificial molecular systems would be incomplete without the development of the fully controllable

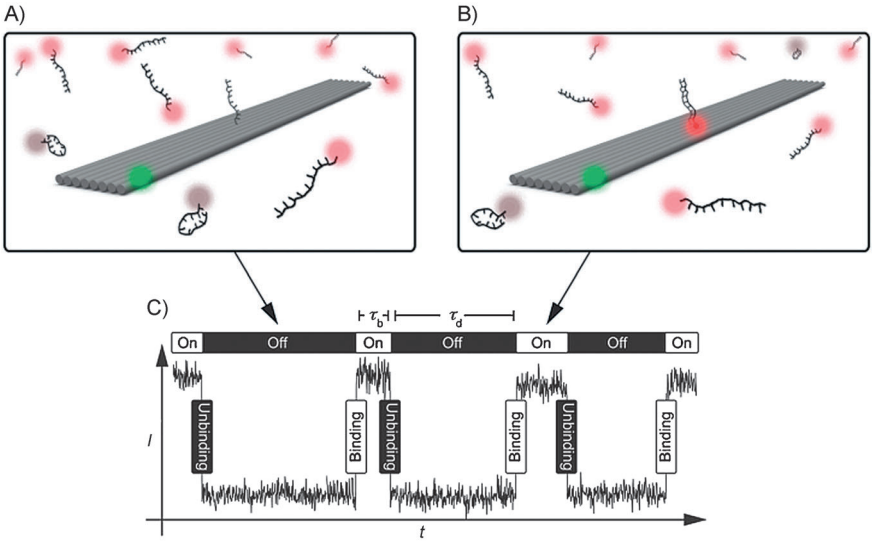

Figure 13. A) The design of an origami tile with a green label dye at the corner and a docking strand in the middle. B) The binding of a red-dye-modified imager strand to the docking strand. C) The fluorescence intensity versus time trace of the binding and unbinding event.

movement of the molecular transporter system.[51] A typical transporter system on the origami surface consists of a track, motor, and fuel, all generated from DNA or a combination of biomacromolecules. Apart from these components, it is also possible to incorporate a control system in the form of preprogrammed machines so that the transport of cargo can be controlled. The speed of the transporter can be fine-tuned by adjusting the spacing between neighboring tracks; alternatively, the transportation can be completely inhibited by adding strands that are complementary to the tracks. Similar to an automobile, the transporter can be designed to carry out a sequence of actions autonomously, such as start, follow, turn, and stop, and these actions can be controlled using external stimuli, inhibitors, or prefunctionalized devices. The DNA tracks on the origami guide the direction of the movement of the transporter. All positional transitions can be performed using the toehold-binding/branch-migration methods. Thermodynamic stabilization energy works as fuel for the mechanical motion of the DNA machines.

Gu et al.[52] created a molecular transporter with three hands and four feet, all of which consist of single-stranded DNA segments (Figure 14A). The hands receive and carry the nanoparticle cargos, which are appropriately placed for pickup. The feet bind to the single strands on the origami surface and allow stepwise movement. In addition to the single-stranded tracks, the origami is designed to have three two-state molecular devices (termed "PX-JX_2 devices"). These devices can rotate two adjacent ends of the duplex DNA by 180° in either the PX (paranemic crossover) or JX_2 state (its topoisomer).[53] They work as control systems that initially hold the cargo species and decide whether the cargo can be transferred to the walker or not. The movements of all devices and of the DNA walker are exclusively controlled by specific DNA strands. Control devices carrying different-sized gold nanoparticle cargos can pass them to the walker by rotational operation when the DNA walker is located nearby. The walker moves in one direction along the track and picks up three different cargos located at three different positions, with a yield of 43% (Figure 14B). Moreover, by changing the two-state molecular devices, it is possible to control the product, with the possibility of eight different final products.

In a parallel study, Lund et al.[54] demonstrated the action of molecular robots guided by prescriptive landscapes. The robot/spider contains a streptavidin molecule as an inner body, a capture strand, and three catalytic legs (Figure 14C). These legs were adapted from the 8–17-DNA enzyme, which hydrolyzes RNA bases. Single-stranded DNA/RNA chimeras were incorporated into the DNA origami, as tracks. These tracks were coded using a sequence of points (a, b, c, d, and e), such that on an a-b-d landscape, the spider starts at a and passes through b before ending at d. The points c and i represent the control sites and topographical imaging marker, respectively. The staple strands at different positions of the track were modified to allow the start, follow, turn, and stop actions. The DNA spider was introduced at the starting position by a capture strand and was then released using a specific DNA strand. The spider migrated along the predetermined track by cleaving the DNA/RNA chimeric strands using the enzyme legs. When the spider reached the stop point, its movement was stopped by the noncleavable DNA strand. The spider movement from a start point to the end stop point through a turn point was captured in AFM images (Figure 14D) and was analyzed unambiguously in real time using superresolution TIRF microscopy. The speed of the spider movement on the DNA origami was estimated at 3 nm min^{-1}.

We developed a DNA transporter that can move along a designed track constructed on a DNA origami and observed the multistep motion of the motor strand.[55] An extended track of 15 identical stators (single-stranded DNAs), flanked by special start and stop stators, was assembled on a rectangular origami (Figure 14E). The stators were the 22-nucleotide sequences extended at the 5′ end of the selected staple strands. The motor was a single-stranded DNA that was complementary to the stator. When the motor strand hybridized to the specific stator at the start point, the hydrolysis of the stator/motor duplex by the Nt.BbvCI restriction enzyme removed the short single-stranded DNA from the stator. The motor strand binds to the next stator by branch migration and steps forward. The process continues until the motor strand reached the end point. The motor strand was imaged as a single spot of the motor/stator duplex. The position of the motor strand before addition of the enzyme and after incubation times of one, two, and three hours was determined using AFM (Figure 14F). The direct

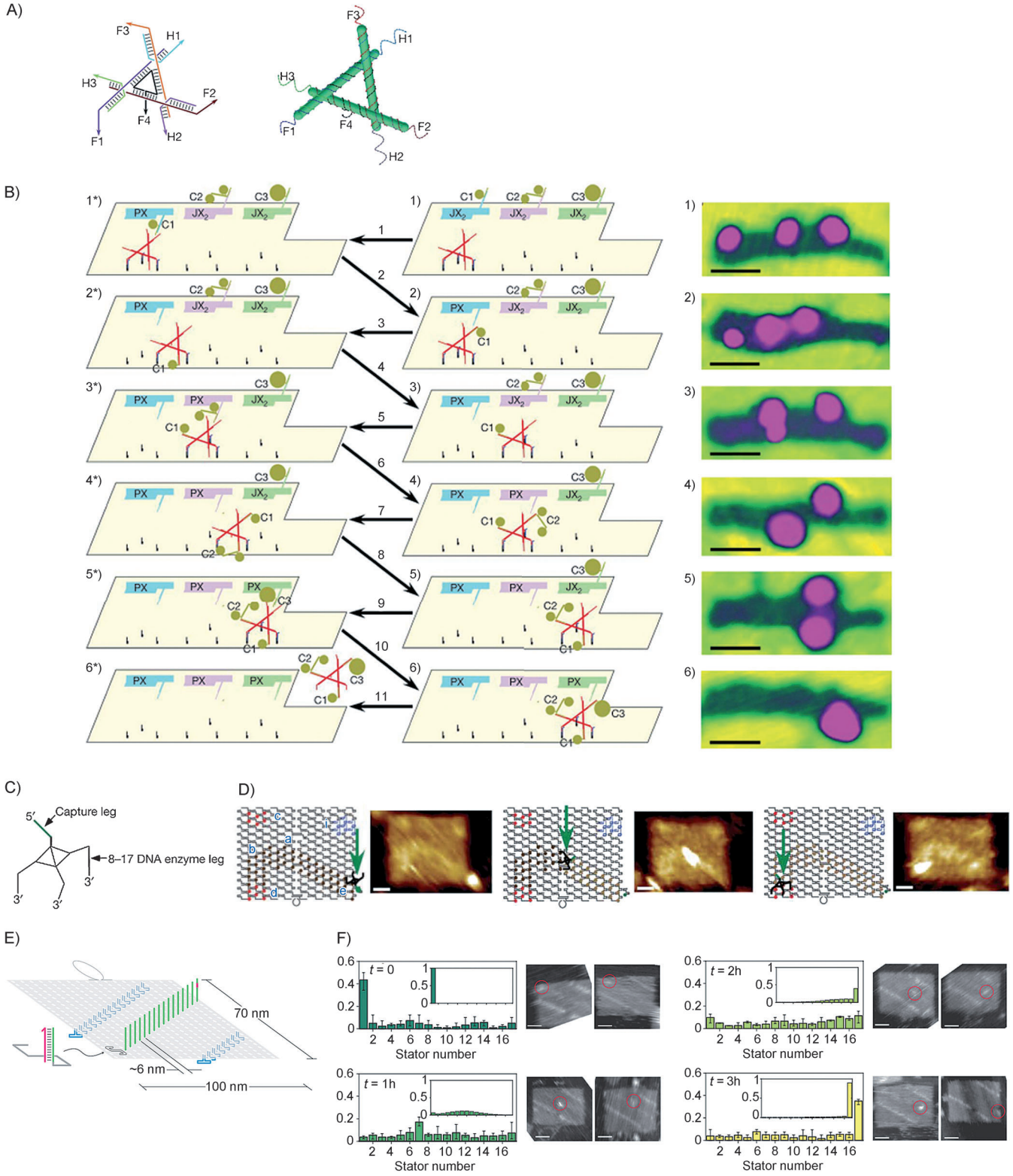

Figure 14. A) Stick figure (left) and strand structure (right) of a walker, indicating the three hands (H1–H3) and four feet (F1–F4). B) The molecular assembly line and its operation (left) and AFM images (right). The origami (pale yellow region), three two-state devices (blue, purple, and green; ON state PX and OFF or nondonating cargo state JX_2), and the walker (triangular arrangement) are the basic components of the system. Cargos are indicated by green-brown dots consisting of 5 nm (C1), coupled-pair 5 nm (C2), and 10 nm (C3) gold nanoparticles. C) The spider consists of a streptavidin core, with a 20-mer single-stranded DNA (green) that positions the spider at the start, and three deoxyribozyme legs. D) Spider movement along the track and AFM images of the spider at the start, on the track, and at the stop sites. Scale bars: 20 nm. E) Layout of the origami tile, bearing the single-stranded stators of the track (green) and two rows of hairpin markers (blue) on opposite surface. F) Seventeen-stator tracks with the motor loaded at stator 1 were incubated with nicking enzyme. The distribution of motor positions before addition of enzyme and after one, two, and three hours were determined by AFM. Representative images and histograms of motor positions are shown (red circles) for each time point. Inset: motor distributions predicted by a simple kinetic model. Scale bars: 20 nm.

observation of the stepwise movement of the motor strand was also performed using high-speed AFM imaging. The spot moved forward along the motor track as revealed by AMF scanning performed every five seconds, and the distance of the motor strand movement corresponded to the distance between the adjacent stators, indicating that the movement occurred in a stepwise manner on the track.

Comparison with protein-based walkers[56] revealed that the transporters reported above were not as fast or efficient. However, as candidates for molecular transporters and robots, these transporters offer programmability, directional specificity, and a highly controllable nature.

8. Conclusions and Outlook

The studies described in this Review show unambiguously that the scaffolded DNA origami method is an extraordinary platform for the placement of a variety of functional molecules and for their single-molecule analysis with the aid of the unimolecular techniques available. The exquisite power of the sequence programmability and structural integrity of DNA-origami-based nanostructures has been used successfully for the precise positioning of numerous molecules and functionalities. Furthermore, these structures have been used for the design of a single-molecule detection array system in aqueous solution that overcomes several disadvantages of the benchtop microarray chip technology. As the method permits analysis in solution, vast physical, chemical, and biochemical studies can be easily performed under the in vivo conditions of such reactions. Moreover, the origami structures are potential candidates for single-molecule investigations, such as distance-dependent and structurally controlled analyses, which cannot be performed using bulk analysis. Regarding the size of the analyte, as mentioned above, it is possible to analyze biomacromolecules with a size of several nanometers, down to chemical reactions that occur on the scale of a few Ångstroms. Size is not a limiting factor in origami-based single-molecule analyses, as even dimensionless physical properties, such as energy transfer, have been successfully studied using this approach. Its timescale is solely dependent on the unimolecular technique that is applied for a particular analysis: Force-based techniques offer analytical speeds of a few seconds; for instance, the high-speed AFM scanning system allows the recording of 15 images per second. Fluorescence-based techniques are superior in terms of speed, as they allow the performance of studies in the subsecond range. In contrast, force-based techniques dominate in terms of the resolution of images (ca. 2 nm) compared with fluorescence imaging.

Despite the advantages offered by origami-based single-molecule analysis, several challenges require clarification before the system can be applied to chemical and biochemical analyses that will culminate in the practical use of liquid-state nanochips. The primary methods that can be used for the expansion of the dimension (typically 1 μm or larger) of the origami are limited, whereas a larger structure may be required to increase the addressability of this system in the patterning of multiple functionalities and to allow simultaneous analyses. Self-assembly can achieve this task efficiently; however, it may be subjected to kinetic and thermodynamic limitations. Liu et al.[15d] described one example of the preparation of a larger 2D origami structure, whereas strategies for the construction of structures with defined size, controllable growth, and higher yield are expected. The stability of the origami structures, which is another important issue, should be improved by means of thermal, chemical, and biochemical resistance, so that the system can be used without limitations in higher-temperature analysis and chemical or enzymatic investigations. We have recently developed a method to thermally stabilize the DNA origami structures.[57] However, a more detailed study is required to explore the different choices of methods. As functional molecules can be placed on the origami, based on their conjugation with single-stranded DNA, the conjugation chemistry for a variety of chemical and biomolecules is now required. The performance of single-molecule analytical techniques requires improvement in terms of spatial resolution and timescale. Although several single-molecule techniques are available, only a few of these techniques have been used to date; in turn, the adoption of additional techniques may lead to a better understanding of unimolecular processes, and we expect that such an inclusion can be performed in the near feature.

In the relatively short time (half a decade) since the first report of the DNA origami method, the creation of various functional structures and their applications to single-molecule analyses has been achieved.[58] The aspects described here are just a starting point, as the field is still in its infancy and is experiencing rapid progress. We anticipate that the strenuous attempts of scientists from different disciplines will result in the building of highly complex autonomous systems for the screening of single-molecule processes.

We express our sincere thanks for a CREST grant from the Japan Science and Technology Corporation (JST), grants from the WPI program (iCeMS, Kyoto University), and for the global COE program from the Ministry of Education, Culture, Sports, Science and Technology (MEXT), Japan. We thank Sekar Latha for her help with the graphics.

Received: March 25, 2011
Published online: November 25, 2011

[1] a) C. Bustamante, *Q. Rev. Biophys.* **2005**, *38*, 291 – 301; b) C. Bustamante, *Annu. Rev. Biochem.* **2008**, *77*, 45 – 50.
[2] P. V. Cornish, T. Ha, *ACS Chem. Biol.* **2007**, *2*, 53 – 61.
[3] a) J. R. Kuhn, T. D. Pollard, *J. Biol. Chem.* **2007**, *282*, 28014 – 28024; b) J. Park, Y. Jeon, D. In, R. Fishel, C. Ban, J-B. Lee, *PLoS One* **2010**, *5*, e15496.
[4] a) A. Camacho, K. Korn, M. Damond, J.-F. Cajot, E. Litborn, B. Liao, P. Thyberg, H. Winter, A. Honegger, P. Gardellin, R. Rigler, *J. Biotechnol.* **2004**, *107*, 107 – 114; b) J. Hasse, J. Jacak, M. Kasper, G. Regl, T. Eichberger, M. Winklmayr, F. Aberger, M. Sonnleitner, R. Schlapak, S. Howorka, L. Muresan, A-M. Frischauf, G. J. Schutz, *Genome Res.* **2006**, *16*, 1041 – 1045; c) K. Korn, P. Gardellin, B. Liao, M. Amacker, A. Bergstrom, H. Bjorkman, A. Camacho, S. Dorhofer, K. Dorre, J. Enstrom, T. Ericson, T. Favez, M. Gosch, A. Honegger, S. Jaccoud, M.

Lapczyna, E. Litborn, P. Thyberg, H. Winter, R. Rigler, *Nucleic Acids Res.* **2003**, *31*, e89.

[5] a) C. R. Twist, M. K. Winson, J. J. Rowland, D. B. Kell, *Anal. Biochem.* **2004**, *327*, 35 – 44; b) P.-Y. Kwok, M. Xiao, *Hum. Mutat.* **2004**, *23*, 442 – 446.

[6] a) J. Sung, S. Sivaramakrishnan, A. R. Dunn, J. A. Spudich, *Methods Enzymol.* **2010**, *475*, 321 – 375; b) T. B. Miranda, T. K. Kelly, K. Bouazoune, P. A. Jones, *Curr. Protoc. Mol. Biol.* **2010**, *89*, 21.17.1 – 21.17.16.

[7] a) M. Hintersteiner, M. Auer, *Ann. N. Y. Acad. Sci.* **2008**, *1130*, 1 – 11; b) G. M. Skinner, K. Visscher, *Assay Drug Dev. Technol.* **2004**, *2*, 397 – 406.

[8] D. Schomburg, I. Schomburg, *Springer Handbook of Enzymes, 2nd ed.*, Springer, New York, **2001**.

[9] M. J. Levene, J. Korlach, S. W. Turner, M. Foquet, H. G. Craighead, W. W. Webb, *Science* **2003**, *299*, 682 – 686.

[10] N. C. Seeman, *J. Theor. Biol.* **1982**, *99*, 237 – 247.

[11] a) K. Lund, Y. Liu, S. Lindsay, H. Yan, *J. Am. Chem. Soc.* **2005**, *127*, 17606 – 17607; b) S. H. Park, C. Pistol, S. J. Ahn, J. H. Reif, A. R. Lebeck, C. Dwyer, T. H. LaBean, *Angew. Chem.* **2006**, *118*, 749 – 753; *Angew. Chem. Int. Ed.* **2006**, *45*, 735 – 739; c) A. Chworos, I. Severcan, A. Y. Koyfman, P. Weinkam, E. Oroudjev, H. G. Hansma, L. Jaeger, *Science* **2004**, *306*, 2068 – 2072.

[12] M. Endo, Y. Katsuda, K. Hidaka, H. Sugiyama, *J. Am. Chem. Soc.* **2010**, *132*, 1592 – 1597.

[13] a) X. D. Cheng, *Annu. Rev. Biophys. Biomol. Struct.* **1995**, *24*, 293 – 318; b) B. Youngblood, N. O. Reich, *J. Biol. Chem.* **2006**, *281*, 26821 – 26831.

[14] P. W. K. Rothemund, *Nature* **2006**, *440*, 297 – 302.

[15] a) Z. Zhao, H. Yan, Y. Liu, *Angew. Chem.* **2010**, *122*, 1456 – 1459; *Angew. Chem. Int. Ed.* **2010**, *49*, 1414 – 1417; b) A. Rajendran, M. Endo, Y. Katsuda, K. Hidaka, H. Sugiyama, *ACS Nano* **2011**, *5*, 665 – 671; c) M. Endo, T. Sugita, A. Rajendran, Y. Katsuda, T. Emura, K. Hidaka, H. Sugiyama, *Chem. Commun.* **2011**, *47*, 3213 – 3215; d) W. Liu, H. Zhong, R. Wang, N. C. Seeman, *Angew. Chem.* **2011**, *123*, 278 – 281; *Angew. Chem. Int. Ed.* **2011**, *50*, 264 – 267.

[16] a) E. S. Andersen, M. Dong, M. M. Nielsen, K. Jahn, R. Subramani, W. Mamdouh, M. M. Golas, B. Sander, H. Stark, C. L. P. Oliveira, J. S. Pedersen, V. Birkedal, F. Besenbacher, K. V. Gothelf, J. Kjems, *Nature* **2009**, *459*, 73 – 76; b) A. Kuzuya, M. Komiyama, *Chem. Commun.* **2009**, 4182 – 4184; c) Y. Ke, J. Sharma, M. Liu, K. Jahn, Y. Liu, H. Yan, *Nano Lett.* **2009**, *9*, 2445 – 2447; d) M. Endo, K. Hidaka, T. Kato, K. Namba, H. Sugiyama, *J. Am. Chem. Soc.* **2009**, *131*, 15570 – 15571; e) M. Endo, K. Hidaka, H. Sugiyama, *Org. Biomol. Chem.* **2011**, *9*, 2075 – 2077; f) S. M. Douglas, H. Dietz, T. Liedl, B. Hogberg, F. Graf, W. M. Shih, *Nature* **2009**, *459*, 414 – 418; g) H. Dietz, S. M. Douglas, W. M. Shih, *Science* **2009**, *325*, 725 – 730; h) Y. Ke, S. M. Douglas, M. Liu, J. Sharma, A. Cheng, A. Leung, Y. Liu, W. M. Shih, H. Yan, *J. Am. Chem. Soc.* **2009**, *131*, 15903 – 15908.

[17] a) R. Chhabra, J. Sharma, Y. Ke, Y. Liu, S. Rinker, S. Lindsay, H. Yan, *J. Am. Chem. Soc.* **2007**, *129*, 10304 – 10305; b) W. Shen, H. Zhong, D. Neff, M. L. Norton, *J. Am. Chem. Soc.* **2009**, *131*, 6660 – 6661; c) A. Kuzyk, K. T. Laitinen, P. Torma, *Nanotechnology* **2009**, *20*, 235305 – 235310; d) A. Kuzuya, M. Kimura, K. Numajiri, N. Koshi, T. Ohnishi, F. Okada, M. Komiyama, *ChemBioChem* **2009**, *10*, 1811 – 1815; e) K. Numajiri, M. Kimura, A. Kuzuya, M. Komiyama, *Chem. Commun.* **2010**, *46*, 5127 – 5129.

[18] a) S. Pal, Z. Deng, B. Ding, H. Yan, Y. Liu, *Angew. Chem.* **2010**, *122*, 2760 – 2764; *Angew. Chem. Int. Ed.* **2010**, *49*, 2700 – 2704; b) B. Ding, Z. Deng, H. Yan, S. Cabrini, R. N. Zuckermann, J. Bokor, *J. Am. Chem. Soc.* **2010**, *132*, 3248 – 3249.

[19] a) N. Stephanopoulos, M. Liu, G. J. Tong, Z. Li, Y. Liu, H. Yan, M. B. Francis, *Nano Lett.* **2010**, *10*, 2714 – 2720; b) H. T. Maune, S.-P. Han, R. D. Barish, M. Bockrath, W. A. Goddard III, P. W. K. Rothemund, E. Winfree, *Nat. Nanotechnol.* **2010**, *5*, 61 – 66.

[20] S. M. Douglas, J. J. Chou, W. M. Shih, *Proc. Natl. Acad. Sci. USA* **2007**, *104*, 6644 – 6648.

[21] Y. Ke, S. Lindsay, Y. Chang, Y. Liu, H. Yan, *Science* **2008**, *319*, 180 – 183.

[22] N. V. Voigt, T. Torring, A. Rotaru, M. F. Jacobsen, J. B. Ravnsbaek, R. Subramani, W. Mamdouh, J. Kjems, A. Mokhir, F. Besenbacher, K. V. Gothelf, *Nat. Nanotechnol.* **2010**, *5*, 200 – 203.

[23] S. Helmig, A. Rotaru, D. Arian, L. Kovbasyuk, J. Arnbjerg, P. R. Ogilby, J. Kjems, A. Mokhir, F. Besenbacher, K. V. Gothelf, *ACS Nano* **2010**, *4*, 7475 – 7480.

[24] M. Endo, Y. Katsuda, K. Hidaka, H. Sugiyama, *Angew. Chem. Int. Ed.* **2010**, *49*, 9412 – 9416; also reference [12].

[25] I. H. Stein, C. Steinhauer, P. Tinnefeld, *J. Am. Chem. Soc.* **2011**, *133*, 4193 – 4195.

[26] H. K. K. Subramanian, B. Chakraborty, R. Sha, N. C. Seeman, *Nano Lett.* **2011**, *11*, 910 – 913.

[27] Y. Sannohe, M. Endo, Y. Katsuda, K. Hidaka, H. Sugiyama, *J. Am. Chem. Soc.* **2010**, *132*, 16311 – 16313.

[28] a) C. Steinhauer, R. Jungmann, T. L. Sobey, F. C. Simmel, P. Tinnefeld, *Angew. Chem.* **2009**, *121*, 9030 – 9034; *Angew. Chem. Int. Ed.* **2009**, *48*, 8870 – 8873; b) R. Jungmann, C. Steinhauer, M. Scheible, A. Kuzyk, P. Tinnefeld, F. C. Simmel, *Nano Lett.* **2010**, *10*, 4756 – 4761; see also reference [25].

[29] a) U. R. Mueller, D. V. Nicolau, *Microarray Technology and its Applications*, Springer, Berlin, **2005**; b) M. Schena, D. Shalon, R. W. Davis, P. O. Brown, *Science* **1995**, *270*, 467 – 470.

[30] S. A. Bustin, T. Nolan, *in Real-Time PCR: An Essential Guide* (Eds.: K. Edwards, J. Logan, N. Saunders), Horizon Bioscience, Norfolk, **2004**.

[31] C. E. Castro, F. Kilchherr, D.-N. Kim, E. L. Shiao, T. Wauer, P. Wortmann, M. Bathe, H. Dietz, *Nat. Methods* **2011**, *8*, 221 – 229.

[32] Q. Mei, X. Wei, F. Su, Y. Liu, C. Youngbull, R. Johnson, S. Lindsay, H. Yan, D. Meldrum, *Nano. Lett.* **2011**, *11*, 1477 – 1482.

[33] S. Rinker, Y. Ke, Y. Liu, R. Chhabra, H. Yan, *Nat. Nanotechnol.* **2008**, *3*, 418 – 422.

[34] a) F. S. Collins, M. S. Guyer, A. Chakravarti, *Science* **1997**, *278*, 1580 – 1581; b) A. J. Schafer, J. R. Hawkins, *Nat. Biotechnol.* **1998**, *16*, 33 – 39; c) A-C. Syvanen, *Nat. Rev. Genet.* **2001**, *2*, 930 – 942; d) E. Lai, *Genome Res.* **2001**, *11*, 927 – 929.

[35] a) U. Landegren, M. Nilsson, P-Y. Kwok, *Genome Res.* **1998**, *8*, 769 – 776; b) A. Rajendran, V. Thiagarajan, B. Rajendar, S. Nishizawa, N. Teramae, *Biochim. Biophys. Acta Gen. Subj.* **2009**, *1790*, 95 – 100; c) A. Rajendran, C. Zhao, B. Rajendar, V. Thiagarajan, Y. Sato, S. Nishizawa, N. Teramae, *Biochim. Biophys. Acta Gen. Subj.* **2010**, *1800*, 599 – 610; d) V. Thiagarajan, A. Rajendran, H. Satake, S. Nishizawa, N. Teramae, *ChemBioChem* **2010**, *11*, 94 – 100; e) B. Rajendar, A. Rajendran, Z. Ye, E. Kanai, Y. Sato, S. Nishizawa, M. Sikorski, N. Teramae, *Org. Biomol. Chem.* **2010**, *8*, 4949 – 4959; f) B. Rajendar, A. Rajendran, Y. Sato, S. Nishizawa, N. Teramae, *Bioorg. Med. Chem.* **2009**, *17*, 351 – 359; g) C. Zhao, A. Rajendran, Q. Dai, S. Nishizawa, N. Teramae, *Anal. Sci.* **2008**, *24*, 693 – 695; h) A. Okamoto, K. Tanaka, T. Fukuta, I. Saito, *J. Am. Chem. Soc.* **2003**, *125*, 9296 – 9297; i) K. Nakatani, S. Sando, I. Saito, *Nat. Biotechnol.* **2001**, *19*, 51 – 55.

[36] a) I. G. Panyutin, P. Hsieh, *Proc. Natl. Acad. Sci. USA* **1994**, *91*, 2021 – 2025; b) S. Q. Wang, X. H. Wang, S. H. Chen, W. Guan, *Anal. Biochem.* **2002**, *309*, 206 – 211.

[37] Z. Zhang, Y. Wang, C. Fan, C. Li, Y. Li, L. Qian, Y. Fu, Y. Shi, J. Hu, L. He, *Adv. Mater.* **2010**, *22*, 2672 – 2675.

[38] a) A. Rajendran, S. Nakano, N. Sugimoto, *Chem. Commun.* **2010**, *46*, 1299 – 1301; b) G. Wang, K. M. Vasquez, *Mutat. Res.* **2006**, *598*, 103 – 119.

[39] a) W. E. Wright, V. M. Tesmer, K. E. Huffman, S. D. Levene, J. W. Shay, *Genes Dev.* **1997**, *11*, 2801 – 2809; b) V. L. Makarov, Y. Hirose, J. P. Langmore, *Cell* **1997**, *88*, 657 – 666.

[40] a) J. L. Mergny, C. Helene, *Nat. Med.* **1998**, *4*, 1366 – 1367; b) S. Neidle, G. Parkinson, *Nat. Drug Discov.* **2002**, *1*, 383 – 393; c) L. H. Hurley, *Nat. Rev. Cancer* **2002**, *2*, 188 – 200.

[41] a) T. Mashimo, H. Yagi, Y. Sannohe, A. Rajendran, H. Sugiyama, *J. Am. Chem. Soc.* **2010**, *132*, 14910 – 14918; b) Y. Sannohe, H. Sugiyama, *Curr. Protoc. Nucl. Acid Chem.* **2010**, *40*, 17.2.1 – 17.2.17; see also references [39] and [40].

[42] a) Z. Yang, J. F. Carey, J. J. Champoux, *FEBS J.* **2009**, *276*, 5906 – 5919; b) S. Shuman, D. G. Bear, J. Sekiguchi, *EMBO J.* **1997**, *16*, 6584 – 6589; c) A. Patel, L. Yakovleva, S. Shuman, A. Mondragon, *Structure* **2010**, *18*, 725 – 733.

[43] R. Subramani, S. Juul, A. Rotaru, F. F. Andersen, K. V. Gothelf, W. Mamdouh, F. Besenbacher, M. Dong, B. R. Kundsen, *ACS Nano* **2010**, *4*, 5969 – 5977.

[44] C. W. Tornoe, C. Christensen, M. Meldal, *J. Org. Chem.* **2002**, *67*, 3057 – 3064.

[45] H. C. Kolb, M. G. Finn, K. B. Sharpless, *Angew. Chem.* **2001**, *113*, 2056 – 2075; *Angew. Chem. Int. Ed.* **2001**, *40*, 2004 – 2021.

[46] H. Liu, T. Torring, M. Dong, C. B. Rosen, F. Besenbacher, K. V. Gothelf, *J. Am. Chem. Soc.* **2010**, *132*, 18054 – 18056.

[47] S. E. Halford, J. F. Marko, *Nucleic Acids Res.* **2004**, *32*, 3040 – 3052.

[48] S. W. Hell, *Nat. Methods* **2009**, *6*, 24 – 32.

[49] a) R. B. Best, K. A. Merchant, I. V. Gopich, B. Schuler, A. Bax, W. A. Eaton, *Proc. Natl. Acad. Sci. USA* **2007**, *104*, 18964 – 18969; b) B. Schuler, E. A. Lipman, P. J. Steinbach, M. Kumke, W. A. Eaton, *Proc. Natl. Acad. Sci. USA* **2005**, *102*, 2754 – 2759; c) M. J. Rust, M. Bates, X. Zhuang, *Nat. Methods* **2006**, *3*, 793 – 796; d) T. Heinlein, A. Biebricher, P. Schlueter, C. M. Roth, D.-P. Herten, J. Wolfrum, M. Heilemann, C. Mueller, P. Tinnefeld, M. Sauer, *ChemPhysChem* **2005**, *6*, 949 – 955.

[50] I. H. Stein, V. Schuller, P. Bohm, P. Tinnefeld, T. Liedl, *ChemPhysChem* **2011**, *12*, 689 – 695.

[51] For representative examples: a) R. Siegwart, I. R. Nourbakhsh, *Introduction to Autonomous Mobile Robots*, MIT Press, USA, **2004**; b) J.-S. Shin, N. A. Pierce, *J. Am. Chem. Soc.* **2004**, *126*, 10834 – 10835; c) W. B. Sherman, N. C. Seeman, *Nano Lett.* **2004**, *4*, 1203 – 1207.

[52] H. Gu, J. Chao, S-J. Xiao, N. C. Seeman, *Nature* **2010**, *465*, 202 – 205.

[53] a) H. Yan, X. Zhang, Z. Shen, N. C. Seeman, *Nature* **2002**, *415*, 62 – 65; b) S. Liao, N. C. Seeman, *Science* **2004**, *306*, 2072 – 2074.

[54] K. Lund, A. J. Manzo, N. Dabby, N. Michelotti, A. Johnso *n*Buck, J. Nangreave, S. Taylor, R. Pei, M. N. Stojanovic, N. G. Walter, E. Winfree, H. Yan, *Nature* **2010**, 465, 206 – 210.

[55] S. F. J. Wickham, M. Endo, Y. Katsuda, K. Hidaka, J. Bath, H. Sugiyama, A. J. Turberfield, *Nat. Nanotechnol.* **2011**, *6*, 166 – 169.

[56] H. Hess, *Science* **2006**, *312*, 860 – 861.

[57] A. Rajendran, M. Endo, Y. Katsuda, K. Hidaka, H. Sugiyama, *J. Am. Chem. Soc.* **2011**, *133*, 14488 – 14491..

[58] B. Saccà, C. M. Niemeyer, *Angew. Chem.*, DOI: 10.1002/ange.201105846; *Angew. Chem. Int. Ed.*, DOI: 10.1002/anie.201105846.